

Cell Reports Medicine, Volume 4

Supplemental information

Tracer metabolomics reveals the role of aldose reductase in glycosylation

Silvia Radenkovic, Anna N. Ligezka, Sneha S. Mokashi, Karen Driesen, Lynn Dukes-Rimsky, Graeme Preston, Luckio F. Owuocha, Leila Sabbagh, Jehan Mousa, Christina Lam, Andrew Edmondson, Austin Larson, Matthew Schultz, Pieter Vermeersch, David Cassiman, Peter Witters, Lesa J. Beamer, Tamas Kozicz, Heather Flanagan-Steet, Bart Ghesquière, and Eva Morava

Supplemental Data
 Supplementary Tables and Figures

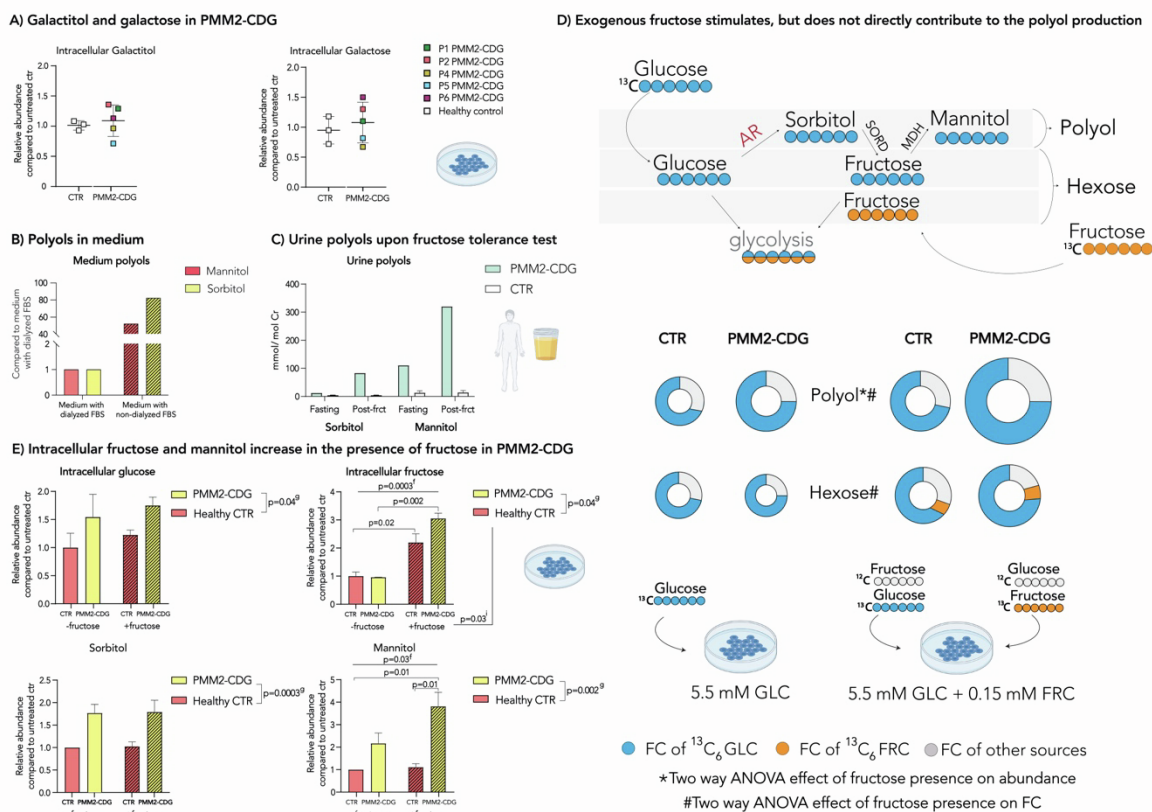
ID	Gene	Nucleotide change	Age#/Gender	Highest measured urine Sorbitol <5 mmol/mol CT	Highest measured urine Mannitol <20 mmol/mol CT
P1	<i>PMM2</i>	c.422G>A, c.722G>C	26/F	7	23
P2*+	<i>PMM2</i>	c.422G>A; c.338C>T	47/F	41	69
P3*+	<i>PMM2</i>	c.422G>A; c.338C>T	47/F	41	113
P4*	<i>PMM2</i>	c.422G>A, c.647A>T	9/M	5.67	121.74
P5*	<i>PMM2</i>	c.415G>A, c.422G>A	9/F	19.93	648.6
P6*	<i>PMM2</i>	c.422G>A, c.548T>C	8/M	50.80	23.90
P7	<i>PMM2</i>	c.422G>A, c.647A>T	3/F	9.85	10.37
P8*	<i>PMM2</i>	c.357C>A, c.422G>A	9/M	130.53	194.13
P9*	<i>PMM2</i>	c.422G>A, c.203T>G	3/M	12.76	9.01
P10*	<i>PMM2</i>	c.109C>T, c.337C>A	4/M	24.23	52.94
P11*	<i>PMM2</i>	c.98A>C, c.140C>T	11/M	3	6
P12*	<i>PMM2</i>	c.422G>A, c.722G>C	14/M	12.45	16.44
P13*	<i>PMM2</i>	c.422G>A, c.458T>C	18/M	3.99	3.64
P14*	<i>PMM2</i>	c.368G>A, c.722G>C	25/F	5.74	12.04
P15*	<i>PMM2</i>	c.647A>G; c.415G>A	71/M	2.80	7.99
P16*	<i>PMM2</i>	c.422 G>A, c.640-23A>G	13/F	5.86	22.55
P17*	<i>PMM2</i>	c.422 G>A, c.640-23A>G	11/M	30.09	89.87
P18*	<i>PMM2</i>	c.338C>T, c.422G>A	10/M	5.16	6.96
P19*	<i>PMM2</i>	c.563A>G, c.691G>A	10/F	14.7	59.2
P20*	<i>PMM2</i>	c.422 G>A, c.385G>A	7/M	14.80	28.46
P21*	<i>PMM2</i>	c.422G>A, c.357C>A	5/M	41.73	46.4
P22*	<i>PMM2</i>	c.385G>A, c.422G>A	6/F	14.65	12.55
P23*	<i>PMM2</i>	c.691G>A, c.422G>A	6/M	19.69	21.09
P24*	<i>PMM2</i>	c.422G>A, c.713G>A	10/M	7.47	33.52
P25*	<i>PMM2</i>	c.422G>A, c.623G>C	12/F	2.69	7.03
P26	<i>PMM2</i>	c. 422G>A, c.686A>C	15/F	14.68	14.85
P27	<i>PMM2</i>	c.422G>A, c.722G>C	21/F	5.65	8.48
P28	<i>PMM2</i>	c.323C>T, c.710C>G	15/M	11.87	9.52
P29	<i>PMM2</i>	c.422G>A, c.44G>C	4/M	12.79	13.65
P30	<i>PMM2</i>	c.323C>T, c.710C>G	11/M	5.19	8.66
P31	<i>PMM2</i>	c.26G>A, c.442G>A	26/M	1.03	2.52
P32	<i>PMM2</i>	c.710C>G, c.728T>C	2/F	13.12	5.57
P33	<i>PMM2</i>	c.422G>A, c.691G>A	10/M	8.49	138.29
P34	<i>PMM2</i>	c.323C>T, c.422G>A	4/M	8.33	10.20
P35	<i>PMM2</i>	c.548T>C	5/M	10.36	10.20
P36	<i>PMM2</i>	c.422G>A, c.556G>A	9/F	11.46	19.66
P37	<i>PMM2</i>	c.470T>C, c.710C>T	15/M	9.8	66.6
P38	<i>PMM2</i>	c.422G>A, c.338C>T	16/M	5.13	10.19
P39	<i>PMM2</i>	c.205 C>T, c.442G>A	10/M	5.36	8.68
P40	<i>PMM2</i>	c.357C>A, c.639-1G>T	27/M	6.27	5.72
P41	<i>PMM2</i>	c.442G>A, c.338C>T	9/M	13.25	47.51
P42	<i>PMM2</i>	c.422G>A, c.337C>T	10/M	5.55	9.28
P43	<i>PMM2</i>	c.458T>C, c.43G>A	3/F	7.13	30.32

Tracer metabolomics reveals the role of aldose reductase in glycosylation

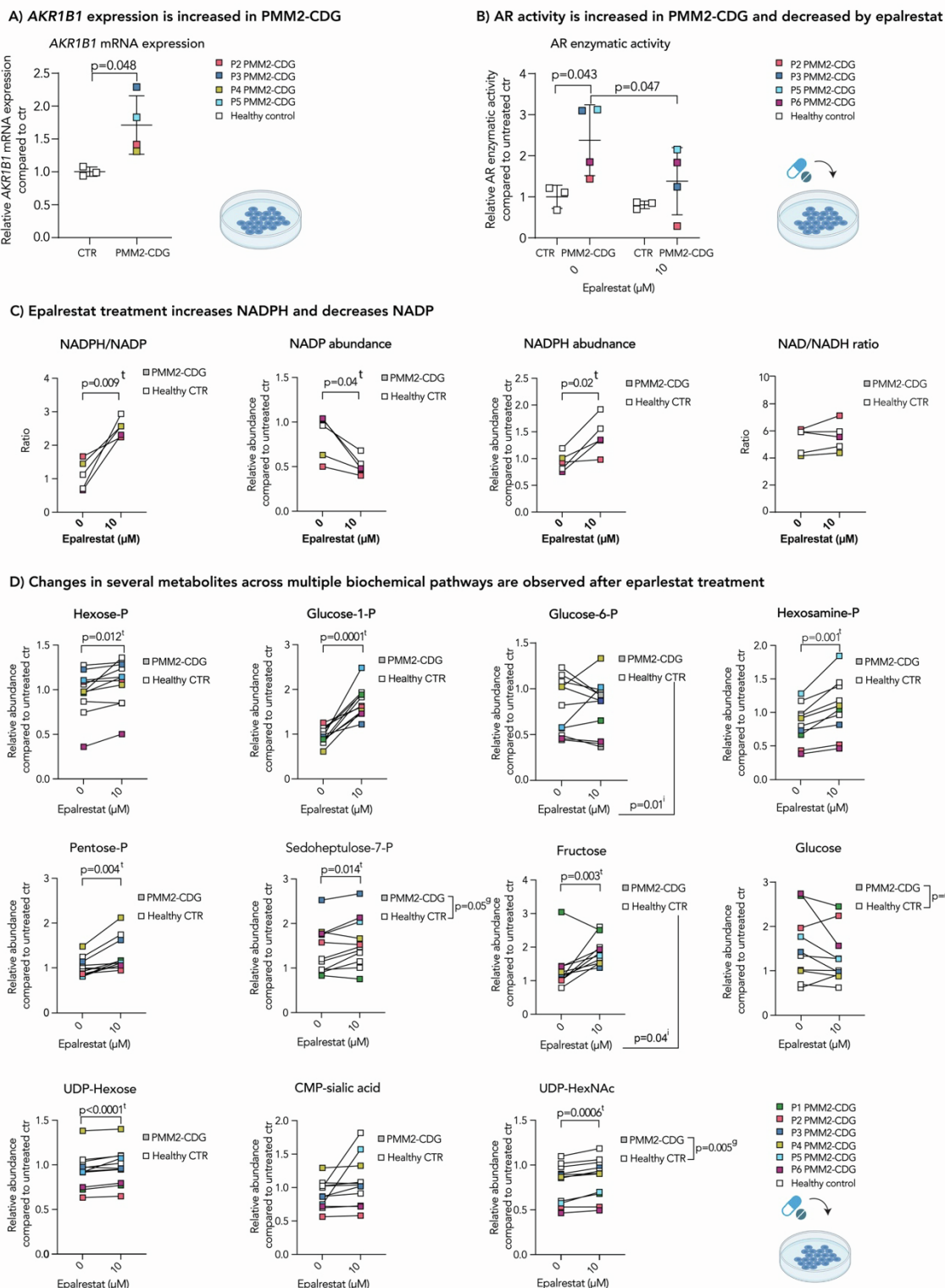
Radenkovic *et al*, 2023

P44	<i>PMM2</i>	c.422G>A, c.647A>T	5/F	8.58	10.46	
P45	<i>PMM2</i>	c.722G>C, c.710 C>G	8/F	5.05	17.71	
P46[^]	<i>PMM2</i>	c.357C>A	35/F	8.44	39.63	
P47	<i>PMM2</i>	c.422G>A, c.707A>G	4/F	20.64	163.32	
P48	<i>PMM2</i>	c.422G>A, c.647A>T	4/M	17.82	160.78	
P49	<i>PMM2</i>	c.95_96delTAinsGC, c.422G>A	11/F	56.79	39.83	
P50	<i>PMM2</i>	c.422G>A, c.524-5G>A intronic	3m/M	14.62	17.94	
PMM enzymatic activity assay in patient fibroblasts supplemented with 10 μM epalrestat^s						
ID				PMM FC	MPI FC	
P2*+	<i>PMM2</i>	c.422G>A; c.338C>T		1.36	0.81	
P3*+	<i>PMM2</i>	c.422G>A; c.338C>T		0.93	1.14	
P4*	<i>PMM2</i>	c.422G>A, c.647A>T		1.35	0.97	
P5*	<i>PMM2</i>	c.415G>A, c.422G>A		1.2	0.86	
P6*	<i>PMM2</i>	c.422G>A, c.548T>C		1.33	1.06	
		average	FC	1.24	0.96	
Thermal shift assay of PMM2 WT and mutant (F119L HOM) protein						
T0.5	CTR1	0.5 mM G16P2	1mM G16P2	5mM G16P2	CTR2	Epalrestat
WT	51.2 °C	56.8 °C	58.6 °C	61.2 °C	51.4 °C	51.6 °C
PMM2						
MUT	45.2 °C	46.2 °C	48.9 °C	53.7 °C	45.3 °C	46.1 °C
PMM2						

Supplementary Table 1. Demographic, genetic, and biochemical characteristics of the patients screened for urine polyols. Related to “disturbed polyol metabolism is a hallmark of PMM2-CDG” result section, Fig 1 and Fig 2. Highest measured urine sorbitol (normal <5 mmol/mmol creatine), mannitol (normal <20 mmol/mmol creatine). Mono-oligo/di-oligo ratio (normal <=0.06); A-oligo/di-oligo ratio (normal <=0.011). Abnormal values are in bold. **PMM enzymatic activity assay.** PMM and MPI enzymes were measured in patient fibroblasts in the presence and absence of 10 μM epalrestat (see methods, previously reported in¹⁹). **Thermal shift assay of PMM2 WT and mutant (F119L HOM) protein.** TS of PMM2 protein wt and mutant (mut) was measured in presence of glucose-1,6-P2 (G16P2), or 10 μM epalrestat. TS is considered significant if > 1°C. **Abbreviations:** ATIII- antithrombin III; ctr- control; F- female; FC- fold change; G16P2- glucose-1,6-P2, M-male; m- months.; P1-50- patient 1-50; wt- wildtype; mut- mutant; # age at the time of the publication (years); & patient on Kepra that contains sorbitol, however, the amounts do not account for the increase seen in urine. \$- results previously reported in¹⁹; +patients first reported in⁶⁰; *patients reported in¹⁹; ^ patient reported in⁶¹



Supplementary Figure 1. Polyol metabolites and the effect of environment on polyol levels related to Result section “Intracellular polyols are elevated in PMM2-CDG regardless of the environment” and Fig 1. A) Intracellular galactitol and galactose in PMM2-CDG fibroblasts. Related to Intracellular polyols are elevated in PMM2-CDG regardless of the environment result section. Galactitol and galactose were measured by GC/MS. PMM2-CDG n=5 (t=1-3), healthy control fibroblasts n=3 (t=1-3). B) Non-dialyzed FBS contains high amounts of mannitol and sorbitol. Sorbitol and mannitol were measured in medium containing dialyzed or non-dialyzed FBS by GC/MS. Relative abundance is shown. C) Urine polyols increase upon fructose tolerance test in PMM2-CDG but not healthy controls. Urine polyols were collected from PMM2-CDG and healthy control before and after fructose administration (PMM2-CDG P5, CTR n=2). D) Fructose stimulates, but does not directly contribute to the increased polyol production in PMM2-CDG. Patient and control fibroblasts were grown in the presence of A) 5.5 mM $^{13}\text{C}_6$ -glucose or B) 5.5mM $^{12}\text{C}_6$ -glucose; C) 5.5 mM $^{13}\text{C}_6$ -glucose and 0.15 mM $^{12}\text{C}_6$ -fructose D) 5.5 mM $^{12}\text{C}_6$ -glucose and 0.15 mM $^{13}\text{C}_6$ -fructose. Abundance (represented by the size of the donut) and fractional contribution of $^{13}\text{C}_6$ glucose/ $^{13}\text{C}_6$ fructose (represented by the blue/orange color of the donut) of polyol and hexose pools with and without addition of 0.15 mM fructose. Polyol and Hexose abundances measured by LC/MS (PMM2-CDG n=1, t=2-6 independent measurements; CTR n=1, t=2-6 independent measurements). E) Intracellular fructose and mannitol increase in the presence of fructose in PMM2-CDG. Patient and control fibroblasts were grown in the presence of A) 5.5 mM glucose or B) 5.5 mM glucose and 0.15 mM fructose. Sorbitol, Mannitol, Glucose and Fructose measured by GC/MS. PMM2-CDG n=1, t=2 independent measurements, healthy control (CTR) n=1, t=2 independent measurements. Relative metabolite abundances were calculated based on the average of untreated CTR treated. FC of was $^{13}\text{C}_6$ glucose and $^{13}\text{C}_6$ fructose was calculated for each metabolite based on the isotopologues distribution and corrected for naturally occurring ^{13}C isotopes (see method section). Detailed results of statistical analysis can be found in Data S1. *note: hexose pool measured by LC/MS contains glucose, fructose, mannose and galactose. All metabolite abundances are represented as relative compared to the untreated control samples. Abbreviations- AR- aldose reductase; CR- creatine; CTR- control; FBS- fetal bovine serum; FC- fractional contribution; MDH- mannitol dehydrogenase, SORD- sorbitol dehydrogenase; P1-6 patient 1-6; g- p-value reflecting the effect of the genotype; i- p-value reflecting the effect of interaction between presence of fructose and genotype, f- p-value reflecting the effect of fructose as calculated by two-way repeated measures anova with post-hoc Sidak correction. The number of biological (n) and technical (t) replicates is given separately for each graph.



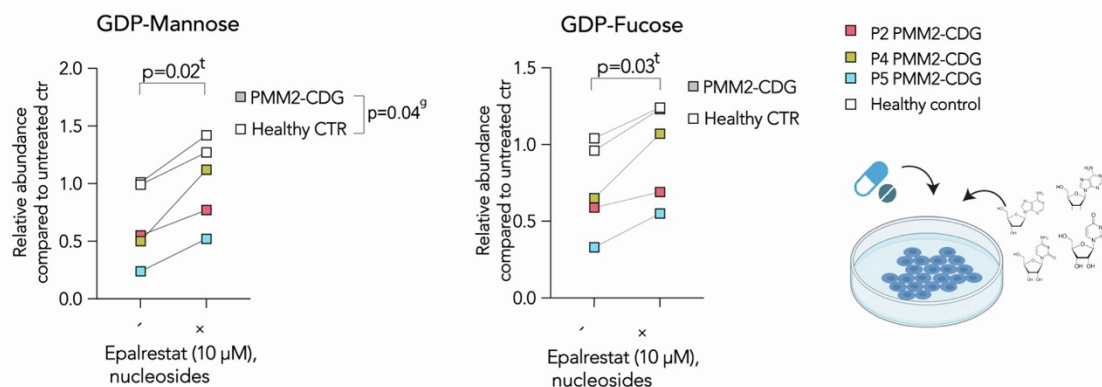
Supplementary Figure 2. Epalrestat supplementation leads to an increase in several metabolites across multiple biochemical pathways. Related to Fig 2. A) AKR1B1 gene expression is increased in PMM2-CDG fibroblasts in the presence of physiological glucose. RT-qPCR was performed to assess *AKR1B1* gene expression. Relative *AKR1B1* mRNA expression compared to the average of healthy control is shown. PMM2-CDG (n=4, t=1) and healthy control fibroblasts (n=3, t=1) showed increased *AKR1B1* in the presence of 5.5mM (physiological) glucose. **B) AR enzymatic activity is increased in PMM2-CDG and decreased in the presence of epalrestat.** Relative AR enzymatic activity was measured in PMM2-CDG (n=4, t=1) and healthy control fibroblasts (n=3, t=1) by AR activity assay kit. **C) AR inhibition results in an increase in**

Tracer metabolomics reveals the role of aldose reductase in glycosylation

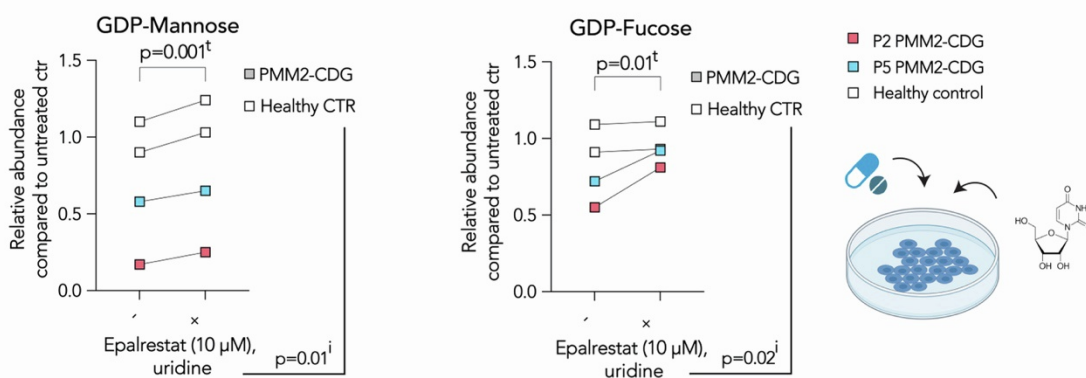
Radenkovic *et al*, 2023

NADPH/NADP. NADPH/NADP ratio increases after epalrestat treatment. NADP abundance is decreased, while NADPH abundance increases after epalrestat treatment. NAD/NADH likewise increases upon epalrestat treatment, however the changes are not as significant as NADPH/NADP. PMM2-CDG n=3, healthy control n=2, t=1. **D)** Changes in several metabolites are observed in the presence of epalrestat in PMM2-CDG patient fibroblasts. Hexose-P (Hex-P), glucose-1-P, glucose-6-P, UDP-Hexose; Hexosamine-P, UDP-HexNAc, CMP-sialic acid, pentose-P (pool of ribose-5-P, ribose-1-P, etc.); sedoheptulose-7-P. PMM2-CDG n=6, t=2-4; healthy control n=5, t=1-4. Fructose and glucose PMM2-CDG n=6, t=1-2; healthy control n=4, t=1-2. Welch t-test or two-way repeated measures ANOVA with Sidak correction were used for statistical analysis. Detailed summary of statistical analyses can be found in **data S1**. *AKR1B1* expression, AR enzymatic activity and all metabolite abundances are represented as relative compared to the untreated control samples. **Abbreviations-** AR- aldose reductase CTR- control, P1-6- Patient 1-6; P-phosphate; g- p-value reflecting effect of genotype; t- p-value reflecting the effect of the epalrestat treatment, i- p-value reflecting interaction between treatment and genotype calculated by two-way repeated measures anova. The number of biological (n) and technical (t) replicates is given separately for each graph.

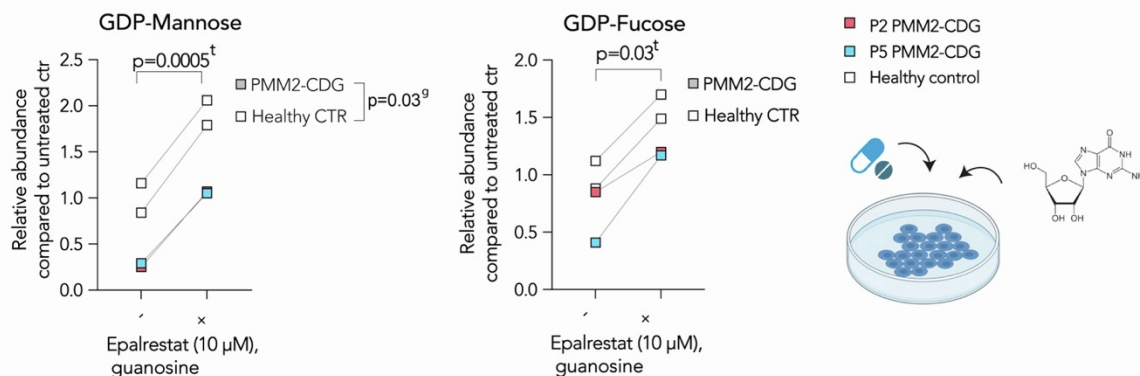
A) Combination treatment of nucleosides and epalrestat



B) Combination treatment of uridine and epalrestat



C) Combination treatment of guanosine and epalrestat



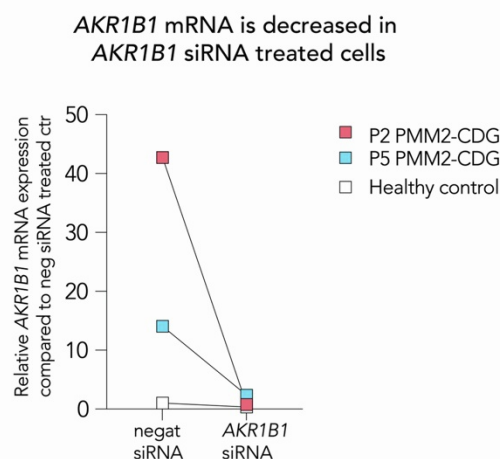
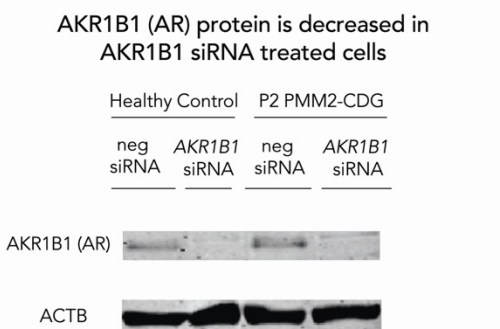
Supplementary Figure 3. Treatment with nucleosides, especially guanosine, increases GDP-mannose abundance in PMM2-CDG. Related to “Treatment with nucleosides, specifically guanosine, increases GDP-mannose abundance in PMM2-CDG to the levels seen in healthy controls” results section and Fig 2. **A) Combination treatment of nucleosides and epalrestat treatment increases GDP-mannose and GDP-fucose abundances.** Patient and control fibroblasts were supplemented with nucleotides (30 μ M each) and 10 μ M epalrestat. We found that the abundance of GDP-mannose and GDP-fucose further increased after the combination therapy of epalrestat and nucleosides compared to epalrestat alone (Figure 2). (PMM2-CDG n=3, t=1; CTR n=2, t=1) **B) Combination treatment of uridine and epalrestat increases GDP-sugar nucleotides.** 30 μ M uridine was supplemented in combination with epalrestat and resulted in a significant increase of GDP-mannose and GDP-fucose. (PMM2-CDG n=2, t=1, CTR n=2, t=1). **C) Combination treatment of guanosine and epalrestat treatment increases GDP-sugar nucleotides to the levels of healthy controls.** 30 μ M guanosine was supplemented in combination with epalrestat and resulted in an increase of GDP-mannose and

Tracer metabolomics reveals the role of aldose reductase in glycosylation

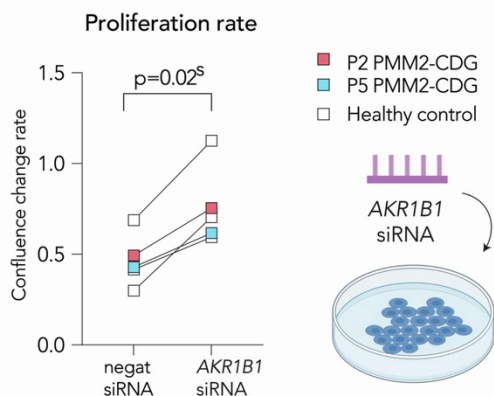
Radenkovic *et al*, 2023

GDP-fucose to the levels seen in healthy controls. (PMM2-CDG n=2, t=1; CTR n=2, t=1). Two-way repeated measures ANOVA was used for statistical analysis. Detailed summary of statistical analyses can be found in Supplementary data master file 1. All metabolite abundances are represented as relative compared to the untreated control samples. **Abbreviations:** CTR- control, g- p-value reflecting effect of genotype; i- p-value reflecting the interaction of genotype and treatment, t- p-value reflecting effect of treatment as calculated by two-way repeated measures anova. The number of biological (n) and technical (t) replicates is given separately for each graph.

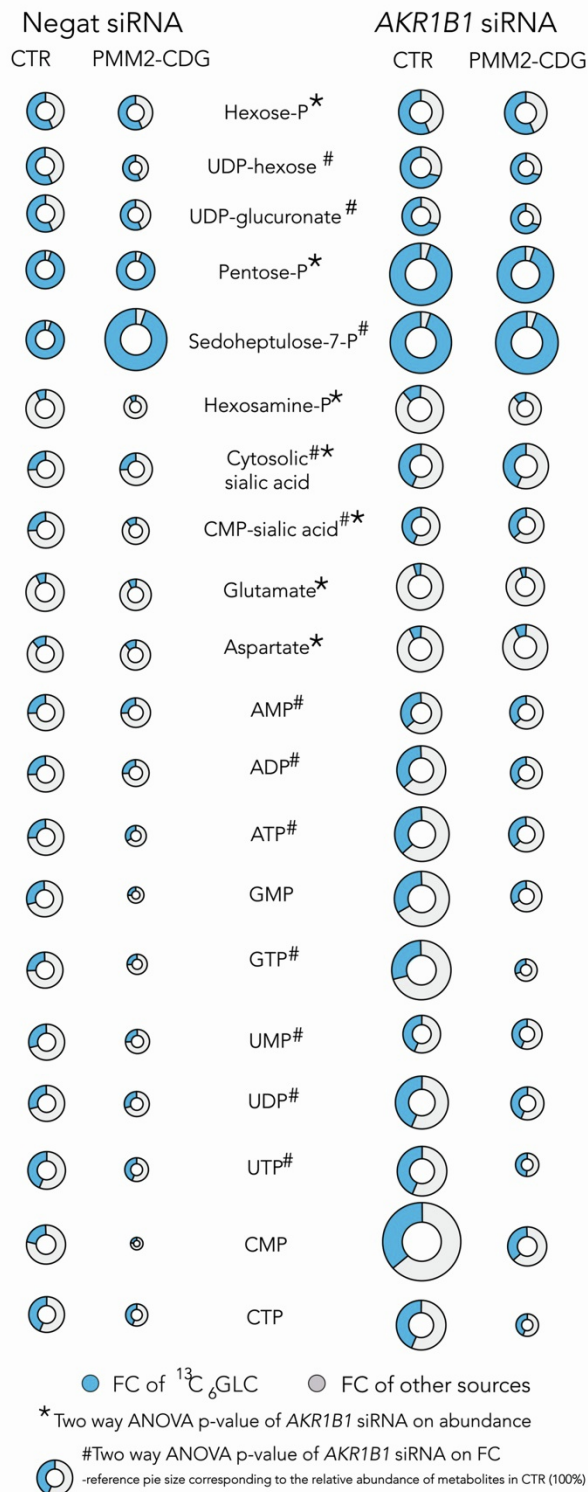
A) Confirmation of AKR1B1 (AR gene) KD



C) AKR1B1 KD results in increased proliferation



B) AKR1B1 siRNA KD results in global metabolic change



Supplementary Figure 4. Effects of AKR1B1 knock-down in healthy and PMM2-CDG cells. Related to Fig 4. **A) Confirmation of AKR1B1 knock down by siRNA targeting AKR1B1.** AKR1B1 (AR) expression was assessed by Western blot (WB) (P2 PMM2-CDG, healthy control) (top panel). AKR1B1 mRNA expression was assessed by AKR1B1 RT-qPCR (P2, P5 PMM2-CDG, t=1; healthy control n=1, t=1) (bottom panel). Relative expression of AKR1B1 mRNA compared to CTR treated with non-targeting (negative) siRNA is shown. **B) siRNA inhibition of AR gene (AKR1B1) results in global metabolic changes.** Both relative abundance (represented by the size of the donut) and fractional contribution (FC) of ¹³C₆ glucose (represented by the blue

Tracer metabolomics reveals the role of aldose reductase in glycosylation

Radenkovic *et al*, 2023

color of the donut) of several metabolites related to glycolysis, TCA, hexosamine biosynthesis, and sugar nucleotide synthesis significantly change upon *AKR1B1* KD. PMM2-CDG n=2, t=2; healthy control n=3, t=1-3. Relative metabolite abundances were calculated based on the average of CTR treated with non-targeting (negative) siRNA. FC of was $^{13}\text{C}_6$ glucose was calculated for each metabolite based on the isotopologues distribution and corrected for naturally occurring ^{13}C isotopes (see method section). Reference size of pie representing average of CTR (100%) is given shown (bottom panel). C) **Inhibition of aldose reductase has a positive effect on cell proliferation.** Confluence change rate was calculated as the difference in the confluence between the first and last day of the experiment, divided by the number of days experiment lasted. Control n=3, t=1, PMM2-CDG n=2, t=1. Two-way repeated measures ANOVA was used for statistical analysis. Detailed summary of statistical analyses can be found **in data S1**. **Abbreviations:** CTR- control, FC- fractional contribution; negat siRNA- negative/non-targeting siRNA, *AKR1B1* siRNA- siRNA targeting *AKR1B1* gene; P- phosphate; * p-value reflecting effect of siRNA *AKR1B1* KD on relative abundance of the metabolite as calculated by two-way repeated measures anova. # p-value reflecting the effect of siRNA *AKR1B1* KD on fractional contribution. The number of biological (n) and technical (t) replicates is given separately for each graph.